THE JOURNAL OF BIOLOGICAL CHEMISTRY VOL. 283, NO. 36, pp. 24781–24788, September 5, 2008

A Functionally Important Hydrogen-bonding Network at the β_{DP}/α_{DP} Interface of ATP Synthase*

Received for publication, May 30, 2008 Published, JBC Papers in Press, June 25, 2008, DOI 10.1074/jbc.M804142200

Hui Z. Mao, Christopher G. Abraham, Arathianand M. Krishnakumar, and Joachim Weber[1]

From the Department of Chemistry and Biochemistry, Texas Tech University, Lubbock, Texas 79409-1061

ATP synthase uses a unique rotary mechanism to couple ATP synthesis and hydrolysis to transmembrane proton translocation. The F_1 subcomplex has three catalytic nucleotide binding sites, one on each β subunit, at the interface to the adjacent α subunit. In the x-ray structure of F_1 (Abrahams, J. P., Leslie, A. G. W., Lutter, R., and Walker, J. E. (1994) *Nature* 370, 621–628), the three catalytic β/α interfaces differ in the extent of inter-subunit interactions between the C termini of the β and α subunits. At the closed β_{DP}/α_{DP} interface, a hydrogen-bonding network is formed between both subunits, which is absent at the more open β_{TP}/α_{TP} interface and at the wide open β_E/α_E interface. The hydrogen-bonding network reaches from βL328 (*Escherichia coli* numbering) and βQ441 via αQ399, βR398, and αE402 to βR394, and ends in a cation/π interaction between βR394 and αF406. Using mutational analysis in *E. coli* ATP synthase, the functional importance of the β_{DP}/α_{DP} hydrogen-bonding network is demonstrated. Its elimination results in a severely impaired enzyme but has no pronounced effect on the binding affinities of the catalytic sites. A possible role for the hydrogen-bonding network in coupling of ATP synthesis/hydrolysis and rotation will be discussed.

F_1F_0-ATP synthase catalyzes the final step of oxidative phosphorylation and photophosphorylation, the synthesis of ATP from ADP and inorganic phosphate. F_1F_0-ATP synthase consists of the membrane embedded F_0 subcomplex with, in *Escherichia coli*, a subunit composition of ab_2c_{10}, and the peripheral F_1 subcomplex, with a subunit composition of $\alpha_3\beta_3\gamma\delta\epsilon$. The energy necessary for ATP synthesis is derived from an electrochemical transmembrane proton (or, in some organisms, sodium ion) gradient. Proton flow, down the gradient, through F_0 is coupled to ATP synthesis on F_1 by a unique rotary mechanism. The protons flow through (half) channels at the interface of a and c subunits, which drives rotation of the ring of c subunits. The c_{10} ring, together with F_1 subunits γ and ϵ, forms the rotor. Rotation of γ leads to conformational changes in the catalytic nucleotide binding sites on the β subunits, where ADP and P_i are bound. The conformational changes result in formation and release of ATP. Thus, ATP synthase converts electrochemical energy, the proton gradient, into mechanical energy in form of subunit rotation and back into chemical energy as ATP. In bacteria, under certain physiological conditions, the process runs in reverse. ATP is hydrolyzed to generate a transmembrane proton gradient, which the bacterium requires for such functions as nutrient import and locomotion (for reviews, see Refs. 1–6).

F_1 (or "F_1-ATPase") has three catalytic nucleotide binding sites, with pronounced differences in their nucleotide binding affinity. The catalytic nucleotide binding sites are located on the β subunits, at the interface to the adjacent α subunit. In the original x-ray structure of bovine mitochondrial F_1 (7), one of the three catalytic sites was filled with the ATP analog AMP-PNP,[2] a second one with ADP (plus azide; see ref. 8), and the third site was empty. Hence, the β subunits are referred to β_{TP}, β_{DP}, and β_E, and the β/α subunit pairs as β_{TP}/α_{TP}, β_{DP}/α_{DP}, and β_E/α_E, respectively. The three catalytic β/α interfaces differ in their degree of interaction between both subunits. The β_{DP}/α_{DP} interface has the most extensive contacts between β and α, the β_{TP}/α_{TP} interface has less, and the β_E/α_E interface has the least. These differences are most pronounced at the C-terminal domains of β and α. Unique to the β_{DP}/α_{DP} interface is an inter-subunit hydrogen-bonding network, reaching from the main-chain oxygen of βL328[3] and the side chain of βQ441 via the side chains of αQ399, βR398, and αE402 to the side chain of βR394. The guanidino group of βR394 forms a cation/π interaction with the phenyl ring of αF406 (Fig. 1, *left-hand panel*). At the β_{TP}/α_{TP} interface, the α-helix carrying residues αQ399, αE402, and αF406 is rotated and has moved away from β by 3–4 Å, preventing all these interactions (Fig. 1, *right-hand panel*). At the β_E/α_E interface, the C-terminal domains of two subunits are even further apart.

The amino acids that make up the hydrogen-bonding network are conserved between bovine mitochondrial ATP synthase and the enzyme from *E. coli*. In the report presented here, we investigate the functional importance of this hydrogen-bonding network at the β_{DP}/α_{DP} interface of *E. coli* ATP synthase by perturbing it to varying degrees by site-directed mutagenesis. Single conservative amino acid substitutions were used to change charges and/or geometry of individual hydrogen bonds, single alanine substitutions removed one, two, or three possible hydrogen bonds, and a triple alanine mutant, βR394A/βR398A/βQ441A, prevented formation of all hydrogen bonds except one, as well as formation of the cation/π interaction. Analysis of the mutants demonstrated the functional impor-

* This work was supported, in whole or in part, by National Institutes of Health Grant GM071462 (to J. W.). The costs of publication of this article were defrayed in part by the payment of page charges. This article must therefore be hereby marked "*advertisement*" in accordance with 18 U.S.C. Section 1734 solely to indicate this fact.

[1] To whom correspondence should be addressed: Texas Tech University, Dept. of Chemistry and Biochemistry, Box 41061, Lubbock, TX 79409-1061. Tel.: 806-742-1297; Fax: 806-742-1289; E-mail: joachim.weber@ttuhsc.edu.

[2] The abbreviation used is: AMPPNP, 5′-adenylyl-β,γ-imidodiphosphate.

[3] *E. coli* residue numbers are used unless indicated otherwise.

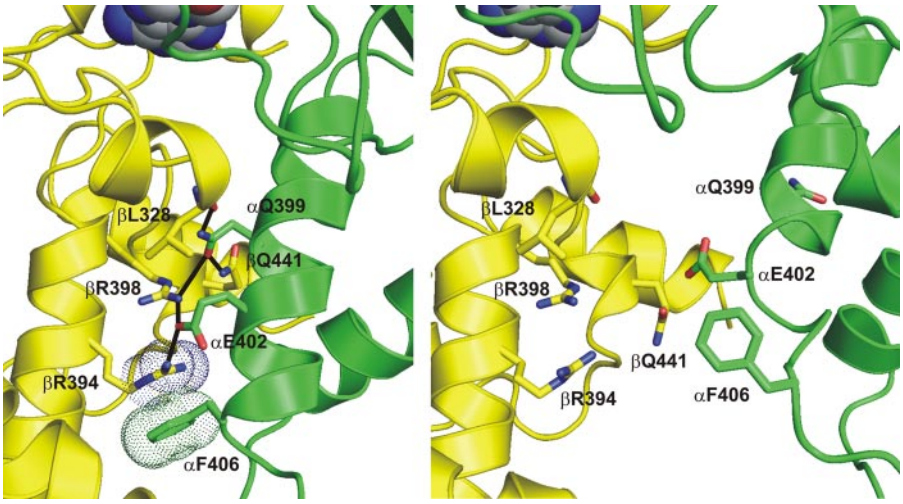

FIGURE 1. **The β_{DP}/α_{DP} hydrogen-bonding network.** The β_{DP}/α_{DP} hydrogen-bonding network is shown in the *left-hand panel*. Protein backbone and selected side-chain carbon atoms of the β subunit are depicted in *yellow*; in the α subunits, these elements are shown in *green*. Oxygen atoms are in *red*, nitrogen atoms in *blue*. The catalytic-site-bound nucleotide is visible at the top of the figure in "*space-fill*" representation. Possible inter-subunit hydrogen bonds are indicated by *black lines*. The "*dots*" represent the van der Waals radii of the guanidino function of βR394 and the phenyl ring of αF406, showing how these groups form a cation/π interaction. For comparison, the *right-hand panel* shows the same residues at the β_{TP}/α_{TP} interface, which lacks the hydrogen-bonding network. The figure was generated using PyMOL (W. L. DeLano (2002) PyMOL, DeLano Scientific, San Carlos, CA).

tance of the hydrogen-bonding network. A possible role for the network in energy coupling will be discussed.

EXPERIMENTAL PROCEDURES

E. coli Strains and Plasmids—The source of wild-type F_1 was strain SWM1 (9), the source of βY331W mutant F_1 was strain pSWM4/JP17 (10). The template for mutagenesis was plasmid pSN6 (11); thus, all new mutants would carry in addition the βY331W mutation, to allow fluorescence-based nucleotide binding measurements. Mutagenesis was performed using the QuikChange II XL kit (Stratagene). The mutagenic oligonucleotides were designed in such a way that, in addition to the desired mutation, a restriction site would be eliminated or generated, to facilitate screening: Plasmids containing the desired mutation were transformed into strain DK8 (12).

Preparation of Membranes and Enzymes and Functional Analysis of Mutant Strains and Enzymes—Growth yields of *E. coli* strains in limiting glucose and growth on succinate plates were measured as described previously (13). *E. coli* membranes were prepared as described (14). F_1 was isolated as described previously (15). NADH- and ATP-driven proton pumping in membranes was measured using acridine orange fluorescence quenching (16). The amount of F_1 in membrane preparations was estimated via Western blots, using an anti-β antibody (Agrisera, Vännäs, Sweden) or an anti-α/anti-β antibody (kindly provided by Dr. Bill Brusilow, Wayne State University). The staining intensity was quantified using a Photodyne imaging system and the program Image J (National Institutes of Health). ATPase activities were measured in 50 mM Tris/H_2SO_4, 10 mM ATP, 4 mM $MgSO_4$, pH 8.0, at 23 °C. Released phosphate was determined as described (17, 18).

Fluorescence Measurements—A general outline of nucleotide binding experiments using βTrp331 fluorescence has been described previously (15). The experiments were performed on a spectrofluorometer type Fluorolog 3 (HORIBA Jovin Yvon, Edison, NJ), at 23 °C. The buffer was 50 mM Tris/H_2SO_4, 2.5 mM $MgSO_4$, pH 8.0. F_1 concentration was 30–60 nM. ATP and ADP were added as indicated. To determine MgADP binding in the presence of scandium fluoride, the enzyme was incubated with 0.3 mM $ScCl_3$, 10 mM NaF, 2.5 mM $MgSO_4$, plus the indicated concentration of ADP (19). To correct for dilution and inner filter effects, parallel titrations with wild-type F_1 were performed. K_d values were determined from the titration curves as described previously (15).

Modeling—Homology modeling, including energy minimization refinement, was performed using the program PRIME (Schroedinger Inc.). Templates were Protein Data Bank entries 1BMF and 1H8E, the structures of bovine mitochondrial F_1 with two (7) and three (20) catalytic sites occupied, respectively. Due to program restrictions regarding the number of amino acids, the N-terminal domains of the α and β subunits were removed.

RESULTS

Assaying the Mutants: An Overview—With the exception of residue βL328, which participates in the β_{DP}/α_{DP} hydrogen-bonding network via its main-chain carbonyl oxygen, the function of the other residues involved in the network was studied by mutational analysis. In addition, residue αF406, which forms a cation/π interaction with one of the terminal residues of the network, βR394, was included in the analysis. The results of the mutagenesis experiments are summarized in Table 1. To characterize the functional effect of each mutation on oxidative phosphorylation *in vivo*, we determined growth yields in 3 mM glucose and growth on plates containing succinate as the sole carbon source. After preparation of membranes from the mutant strains, we analyzed NADH- and ATP-driven proton gradient formation by measuring quenching of acridine orange fluorescence, and we measured ATPase activity. A low percentage of NADH-induced quenching is indicative of proton permeability of the membranes, which can be caused by oligomeric instability of the mutant ATP synthase complex; of the mutations tested here, only the αQ399C mutant showed a pronounced reduction in NADH-induced acridine orange quenching. The degree of quenching by ATP depends on the balance between ATP-driven proton pumping and proton permeability of the membranes. To determine if variations in enzymatic activities were direct functional consequences of the respective mutation or due to changes in the amount of enzyme on the membrane, we quantified the amount of F_1 present in the membrane preparations by Western blots. For most mutants, the amount of F_1 was within ±25% of that observed for the parental

TABLE 1

Functional properties of strains and membranes containing mutations perturbing the β_{DP}/α_{DP} hydrogen-bonding network

Growth yield in limiting (3 mM) glucose and growth on succinate plates were determined as in (13). Growth yield data were measured via the turbidity (A_{590}) and are expressed as percentage of the value for the positive control. Quenching of acridine orange fluorescence by NADH and ATP was measured as in (16). The determination of the amount of F_1 on the membranes is based on the quantitative evaluation of western blots by densitometric analysis (see "Experimental Procedures"). ATPase activities were determined in 50 mM Tris/H_2SO_4, 10 mM ATP, 4 mM $MgSO_4$, pH 8.0, at 23 °C. The relative ATPase activity in the last column is expressed as percentage of the activity of the positive control, corrected for the different amounts of F_1 on the membrane. Strain pSN6/DK8 served as positive control; it expresses ATP synthase containing a βY331W mutation. βY331W mutant ATP synthase is a normal, active enzyme (10, 15, 46). All mutant strains described in the table were derived from strain pSN6/DK8. Strain pUC118/DK8 does not express ATP synthase and served as negative control.

Strain/mutation	Growth yield in limiting glucose	Growth on succinate	Acridine orange quenching		Amount of F_1 on membranes	Membrane ATPase activity	
			NADH-induced	ATP-induced			
	%		%	%	%	*Units/mg*	%
A) Controls							
pSN6/DK8	100	++++	94	85	100	0.55	100
pUC118/DK8 (unc$^-$)	42	−	93	0	0	<0.01	ND[a]
B) Single mutations							
αQ399N	88	+++	84	81	112	0.45	73
αQ399C	46	+	68	0	82	0.02	4
αQ399A	38	−	84	0	0	<0.01	ND
αE402D	76	++	90	54	111	0.31	50
αE402Q	94	+++	92	75	122	0.49	72
αE402A	51	++	90	15	121	0.06	9
αF406W[b]	101[b]						
αF406C[b]	77[b]						
αF406A	48	+	93	6	104	0.18	31
βR394K	58	++	93	21	93	0.13	25
βR394Q	54	++	93	19	88	0.13	27
βR394A	52	++	87	22	107	0.10	17
βR398K	96	+++	91	80	90	0.44	89
βR398H[c]	92[c]	+++					71[c]
βR398Q	92	+++	93	66	107	0.45	76
βR398W[c]	102[c]	++++	91[c]	89[c]			100[c]
βR398C[c]	100[c]	++++	88[c]	85[c]			88[c]
βR398A	89	+++	92	68	88	0.37	76
βQ441N	94	+++	92	79	115	0.40	63
βQ441C	68	++	93	53	151	0.35	42
βQ441A	50	+	88	4	68	0.10	27
C) Triple mutation							
βR394A/βR398A/βQ441A	46	+	91	11	104	0.06	10
S.D.[d]	5		5	10	20	0.05	

[a] ND, not determinable (correction for amount of F_1 leads to division by 0).

[b] Mutations were generated previously.[4] The plasmid containing the αF406W mutation was derived from plasmid pBOW1 (47), encoding ATP synthase with Trp-free F_1. The plasmid containing the αF406C mutation was derived from pBWU13.4 (48), encoding wild-type ATP synthase. Growth yields are given as percentage of the growth yield of the wild-type control (pBWU13.4/DK8). From both mutant strains an active F_1 could be isolated.

[c] Mutations were described previously (34, 35). In all cases, wild-type enzyme was used as background. Growth yields and membrane ATPase activities are expressed as percentage of the respective values for the wild-type control. βR398W mutant F_1 was isolated and showed normal function (49).

[d] Maximum standard deviation for the values in the respective column. All assays were run at least in triplicate, except for the determination of the amount of F_1 on the membrane which was done at least in duplicate.

strain pSN6/DK8. Exceptions were the βQ441A mutant, which had ~2/3 of the F_1 content of the control, the βQ441C mutant, which contained ~50% more F_1 than the control, and the αQ399A mutant, where no F_1 was found on the membrane.

The results of the experiments listed in Table 1 show that the hydrogen-bonding network plays an important role in the function of the enzyme. Many of the mutants showed impaired activity. In most cases, the effect of the mutations on ATP synthesis and hydrolysis was comparable. Although, in general, conservative substitutions had less influence on the enzymatic function less than an alanine replacement, in some cases these differences were smaller than expected. In the following, the results of the mutagenesis experiments will be analyzed in detail.

Mutation of βQ441—The side chain of residue βQ441 can form a hydrogen bond with the side chain of residue αQ399. The mutagenesis results suggest that this hydrogen bond can still be formed when the side chain of βQ441 is shortened by one methylene group to asparagine, because the βQ441N mutant has close-to-normal functional properties. Even the βQ441C mutant seems to have preserved some hydrogen-bonding capabilities. Abolishing the possibility for hydrogen bond formation in the βQ441A mutant impairs the enzyme significantly.

Mutation of αQ399—The side chain of residue αQ399 has a central position in the β_{DP}/α_{DP} hydrogen-bonding network. It can form bonds to the side chains of βQ441 and βR398 as well as to the main-chain carbonyl oxygen of βL328. Like for βQ441, the results of the functional assays suggest that shortening the side chain of αQ399 in the αQ399N mutant leaves the functionally important hydrogen bonds largely unperturbed. Modeling (not shown) of the αQ399N mutation suggested that the hydrogen bonds to the side chains of βQ441 and βR398 might be preserved; in addition, a new hydrogen bond to the hydroxyl group of βY444 seemed possible. Eliminating all potential hydrogen bonds in which the side chain of αQ399 is involved, in the αQ399A mutant, appears to prevent assembly of the enzyme. Visual inspection of the β_{DP}/α_{DP} interaction site indicates that the αQ399C mutant should be capable to form at least one intersubunit hydrogen bond, most likely to βQ441. However, this residual hydrogen-bonding capability does not seem enough

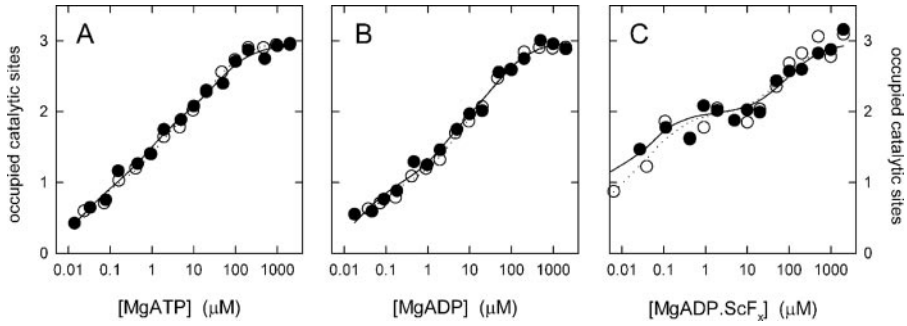

FIGURE 2. **Nucleotide binding to the catalytic sites of βR394A/βR398A/βQ441A mutant F_1.** Nucleotide binding was measured by the decrease in fluorescence of the inserted βW331 residue. *Closed symbols*, βR394A/βR398A/βQ441A+βY331W F_1; *open symbols*, βY331W control. *A*, binding of MgATP; *B*, binding of MgADP; *C*, binding of the transition state analog MgADP·ScF_x. The *lines* are fits of theoretical curves to the measured data points, assuming three independent sites. For the resulting K_d values and further details, see text.

to overcome the loss of the other hydrogen bonds; the αQ399C mutant is very strongly impaired.

Mutation of βR398—The guanidino group of βR398 can form hydrogen bonds with the side chains of αQ399 and αE402, plus an intra-subunit hydrogen bond to the main-chain carbonyl oxygen of βQ441. These hydrogen bonds seem of less importance for the functionality of the enzyme. Even a complete removal in the βR398A mutant gives an enzyme with considerable activity.

Mutation of αE402—The carboxylate group of αE402 can form hydrogen bonds with the guanidino functions of βR398 and βR394. Loss of the negative charge in the αE402Q mutant has only a minor effect on enzymatic function. Shortening the side chain by removal of one methylene group in the αE402D mutant reduces the activity by about a half, possibly by preventing formation of one of the hydrogen bonds. Loss of both hydrogen bonds in the αE402A mutant leaves an enzyme with overall <20% residual activity.

Mutation of βR394—The guanidino group of βR394 can form a hydrogen bond with the carboxylate group of αE402, plus a cation/π interaction with the phenyl ring of αF406. In addition, formation of intra-subunit hydrogen bonds with the hydroxyl function of βY367 and the carboxylate group of βE440 seems likely. Complete removal of the hydrogen-bonding capability in the βR394A mutant reduces the activity severely. Interestingly, in the more conservative mutants, βR394K and βR394Q, a similar decrease in activity was observed. A possible explanation is that the lysine and glutamine side chains preferentially form intra-subunit hydrogen bonds, which are not required for the activity of the enzyme, but fail to provide the functionally important interactions with the α subunit.

Mutation of αF406—The phenyl ring of αF406 can make a cation/π interaction with the guanidino group of βR394. Elimination of this interaction, in the αF406A mutant, results in a significant impairment of the enzyme. Earlier studies[4] had shown that the phenyl ring can be replaced by an indole ring system, in the αF406W mutant, without loss of activity. The αF406C mutant shows considerably higher activity the αF406A mutant, which might suggest that the cation/π interaction between the side chains of αF406 and βR394 has been substituted by a hydrogen bond between the sulfhydryl group of the Cys and the guanidino group of the Arg, with partial preservation of functionality.

The βR394A/βR398A/βQ441A Triple Mutant—In an attempt to remove the β_{DP}/α_{DP} hydrogen-bonding network as completely as possible, without preventing assembly of the enzyme, we constructed a βR394A/βR398A/βQ441A triple mutant. (It is actually a quadruple mutant as the plasmid used to generate the mutations described here contained the βY331W mutation, to allow fluorescence-based nucleotide binding measurements. As described earlier (10), the βY331W mutation gives a normal, fully functional enzyme.) The βR394A/βR398A/βQ441A mutations would eliminate all possible hydrogen bonds plus the cation/π interaction, with the exception of one hydrogen bond between αQ399 and the backbone carbonyl oxygen of βL328. As expected, the data in Table 1 did not give any indication of assembly problems. This is also supported by the fact that we were successful in preparing F_1 from this strain (see below). As can be seen from Table 1, the βR394A/βR398A/βQ441A triple mutant has ~10% residual activity.

F_1 was prepared from the strain containing the βR394A/βR398A/βQ441A triple mutation by the standard procedure (15). The elution profile of the gel chromatography column used as the last purification step indicated that the isolated F_1 subcomplex had normal size and shape. SDS-PAGE of the final product revealed a normal subunit composition (data not shown). The isolated F_1 exhibited ATPase activity of ~10% of that of the parental βY331W enzyme (0.56 unit/mg for βR394A/βR398A/βQ441A+βY331W F_1, as compared with 5.9 units/mg for βY331W mutant F_1; see Refs. 10 and 21).

Nucleotide Binding to the βR394A/βR398A/βQ441A Mutant—The fluorescence of the tryptophan in position β331 was used to determine the affinities for binding of MgATP and MgADP to the three catalytic sites (10, 15). The results of the titrations are shown in Fig. 2 (*A* and *B*). As can be seen, the affinities of βR394A/βR398A/βQ441A+βY331W mutant F_1 do not differ significantly from those of the βY331W control enzyme. For MgATP, the following K_d values were determined: for βR394A/βR398A/βQ441A+βY331W mutant F_1, K_{d1} = 21 nM, K_{d2} = 0.9 μM, K_{d3} = 39 μM; for βY331W mutant F_1, K_{d1} = 20 nM, K_{d2} = 1.5 μM, K_{d3} = 35 μM. For MgADP, the values were as follows: for βR394A/βR398A/βQ441A+βY331W mutant F_1, K_{d1} = 24 nM, K_{d2} = 2.4 μM, K_{d3} = 53 μM; for βY331W mutant F_1, K_{d1} = 28 nM, K_{d2} = 3.6 μM, K_{d3} = 41 μM. These data show that the hydrogen-bonding network, which is present in the βY331W control F_1, but reduced to one possible hydrogen bond in the βR394A/βR398A/βQ441A+βY331W enzyme, does not contribute to the affinity of any of the three catalytic sites. Specifically, it does not increase the affinity of the medium-affinity site 2, which was recently shown to be located on β_{DP} (22).

[4] S. Nadanaciva, J. Weber, and A. E. Senior, unpublished data.

TABLE 2

Conservation of residues forming the β_{DP}/α_{DP} hydrogen-bonding network

Amino acids found in selected species in the position of residues that form the β_{DP}/α_{DP} hydrogen-bonding network in the bovine mitochondrial enzyme (7). Residue numbers refer to the *E. coli* enzyme.

Species	Position					
	β441	α399	β398	α402	β394	α406
Bos taurus	Gln	Gln	Arg	Glu	Arg	Phe
Gallus gallus	Gln	Gln	Arg	Glu	Arg	Phe
Danio rerio (zebrafish)	Gln	Gln	Arg	Glu	Arg	Phe
Drosophila melanogaster	Val	Gln	Arg	Glu	Arg	Phe
Caenorhabditis elegans	Val	Gln	Arg	Glu	Arg	Phe
Saccharomyces cerevisiae	His	Gln	Arg	Glu	Arg	Phe
Neurospora crassa	Gly	Gln	Arg	Glu	Arg	Phe
Arabidopsis thaliana	Gln	Gln	Arg	Glu	Arg	Phe
Spinacia oleracea	Gln	Gln	Arg	Glu	Arg	Phe
Escherichia coli	Gln	Gln	Arg	Glu	Arg	Phe
Clostridium acetobutylicum	Ala	Gln	Arg	Glu	Arg	Phe
Vibrio alginolyticus	Gln	Ala	Arg	Glu	Arg	Phe
Bacillus sp. PS3	Asp	Ala	Phe	Glu	Arg	Phe
Bacillus subtilis	Asp	Ser	Phe	Glu	Arg	Phe
Wolinella succinogenes	Asn	Gln	Lys	Glu	Arg	Phe
Thermotoga maritima	Gln	Gln	Arg	Glu	Arg	Phe
Synechococcus elongatus	Gln	Gln	Lys	Glu	Arg	Phe
Methanosarcina barkeri	Gly	Gln	Arg	Glu	Arg	Phe

$MgADP{\cdot}AlF_x$ and $MgADP{\cdot}ScF_x$ are analogs of the transition state that is formed when MgATP is hydrolyzed to MgADP and P_i. Interestingly, although in F_1 only the high affinity catalytic site 1 is catalytically active (23), a transition-state-like complex forms with $MgADP{\cdot}AlF_x$ and $MgADP{\cdot}ScF_x$ also at the medium affinity site; formation of this complex manifests itself as a significant increase in nucleotide binding affinity (19, 24). Fig. 2*C* shows a titration with MgADP in presence of $ScCl_3$ and NaF. As can be seen from the increased affinities, the $MgADP{\cdot}ScF_x$ complex is generated at sites 1 and 2 also in the absence of the β_{DP}/α_{DP} hydrogen-bonding network. The measured K_d values were as follows: for βR394A/βR398A/βQ441A+βY331W mutant F_1, $K_{d1} < 2$ nM, $K_{d2} = 35$ nM, $K_{d3} = 90$ μM; for βY331W mutant F_1, $K_{d1} < 2$ nM, $K_{d2} = 58$ nM, $K_{d3} = 66$ μM.

Modeling the βR394A/βR398A/βQ441A Mutant—The βR394A/βR398A/βQ441A triple mutant was modeled using either the original structure of bovine mitochondrial F_1 with two occupied catalytic sites (7) or the structure with three occupied catalytic sites (20) as template; in both templates, the conformation of the residues forming the β_{DP}/α_{DP} hydrogen-bonding network is very similar. Except for the "mutated" amino acid side chains, the resulting models (not shown) were very similar to the respective template, and therefore to each other. In both models the hydrogen bond between the main-chain oxygen of βL328 and the side chain of αQ399 were preserved. The geometry between the different secondary structural elements carrying the residues that form the network was not affected by the triple alanine substitution.

Conservation of Residues Forming the β_{DP}/α_{DP} Hydrogen-bonding Network—A BLAST (25) search resulted in several thousand sequences each for α and β subunits of ATP synthase. Of the residues forming the β_{DP}/α_{DP} hydrogen-bonding network, βR394 was completely conserved (see Table 2 for selected species). αE402 and αF406 were conserved in >99% of all species. αF406 was replaced by Leu in some plant mitochondrial ATP synthases. In place of αE402 Asp (~10 cases) and Ser (~5) were found. αQ399 and βR398 were conserved in ~90% of all species. In place of βR398 mostly Lys and Phe were found, in place of αQ399 Ala and Ser. In light of the experimental data obtained here, which indicated that the preservation of two possible hydrogen bonds between αQ399 and β might be required for normal function, the latter result was somewhat surprising. Of the residues under investigation here, βQ441 was the most variable. Replacements that can still form a hydrogen bond were found (Asp, Glu, Ser, Asn, and His) but also others where this is no longer possible (Gly, Ala, and Val).

DISCUSSION

In the study presented here we analyzed the functional importance of an inter-subunit hydrogen-bonding network that is unique to one of the three β/α interfaces in ATP synthase. This hydrogen-bonding network is located between the C-terminal domains of β_{DP} and α_{DP}. Directly involved in formation of inter-subunit contacts via hydrogen bonds are the main-chain carbonyl oxygen of βL328, the sides chain βQ441, αQ399, βR398, αE402, and βR394, plus, via a cation/π interaction, the phenyl ring of αF406 (Fig. 1). This network is present in all published structures of bovine mitochondrial F_1, including the structure with all three catalytic sites occupied by nucleotide (20) and the recent structure obtained in absence of azide (26). Exceptions are the structures that contain the natural inhibitor protein, IF_1 (27, 28). IF_1 is wedged between the C-terminal domains of β_{DP} and α_{DP}, keeping the interface between both subunits more open (more like at the β_{TP}/α_{TP} interface; see Fig. 1), thus preventing formation of the hydrogen-bonding network (27). Instead, residues αQ399, αE402, αF406, and βR394 appear to contribute to binding of the inhibitor protein (27, 28). In the structure of the yeast mitochondrial F_1, the hydrogen-bonding network is present in only one of the three different enzyme conformations; in the two other conformations, the β_{DP}/α_{DP} interface resembled the more open β_{TP}/α_{TP} interface (29). However, as discussed below, there is experimental evidence for the functional importance of some of these residues also in the yeast enzyme. The absence of a comparable hydrogen-bonding network in the recent structure of F_1 from a thermoalkaliphilic *Bacillus* species (30) is not surprising. This structure contains no nucleotide, and all β subunits are in the open conformation, resulting in clefts between the C-terminal domains of β and α at the catalytic interface.

The mutational analysis presented here led to the conclusion that the hydrogen-bonding network is indeed required for normal function of the enzyme. Reduction of the network to a single possible hydrogen bond in the βR394A/βR398A/βQ441A mutant reduced the enzymatic activity to ~10% of normal. Besides the αQ399A mutant, where no ATP synthase was assembled, the single mutants with the overall lowest activities were αQ399C, βQ441A, αF406A, and αE402A, followed by the three βR394 mutants. These findings indicate that the bonds at either end of the network are more important than the central ones (see Fig. 1). On one end, two hydrogen bonds between αQ399 and β seem to be required for normal function; one of them has to be the bond to βQ441. On the other end, the hydrogen bond between αE402 and βR394 plus the cation/π interaction between βR394 and αF406 appear necessary. Ear-

lier results obtained with an αF406C mutant[4] suggest that the cation/π interaction can be replaced by a hydrogen bond.

In general, analysis of the conservation of the residues forming the hydrogen-bonding network confirmed the functional importance of the interactions between αE402 and βR394, and between βR394 and αF406. A possible exception is a group of plant mitochondrial ATPases where αF406 has been replaced by Leu, preventing the cation/π interaction. Unfortunately, the sequences of the β subunits are not known in these cases, making an analysis of the β/α interaction in these enzymes impossible. At the other end of the network, involving positions β441 and α399, a number of cases exist that do not fit into the pattern established here for *E. coli* ATP synthase (see Table 2). Apparently, some enzymes can compensate for the loss of hydrogen bonds from either of these positions. In the case of the thermophilic *Bacillus* sp. PS3 ATP synthase, a part of the hydrogen-bonding network appears to be replaced by hydrophobic interactions. Residue β398 is not an Arg, but a Phe, which can interact with the Leu in position α403. Obviously, an Ala in position α399 fits better into this hydrophobic environment than a Gln. We are planning to characterize the β_{DP}/α_{DP} interactions in the PS3 enzyme by mutational analysis as described here.

Although the present study is the first systematic analysis of the β_{DP}/α_{DP} hydrogen-bonding network, the functional importance of some of the participating residues and their capability to form intra-subunit hydrogen bonds had been noticed before. Mutations that suppress ρ^0-lethality in the yeast *Kluyveromyces lactis* were identified in the genes that code for the α, β, and γ subunits of ATP synthase (31). Among these mitochondrial genome integrity, or *mgi*, mutations (32) found were αF406S,L and βR394G,I,T,V,K (31). None of the mutations abolished the ability of the respective strain to grow on glycerol, and all tested mutations (αF406S and βR394G,K) showed some ATPase activity of isolated mitochondria (31). These results are comparable to those described here for mutations of residues αF406 and βR394. Introduction of a similar set of mutations in *Saccharomyces cerevisiae* (αF406S and βR394G,I) gave similar results (32). In contrast, another study using *S. cerevisiae* (33) found that mutations of residue βR394 (in βR394I,T mutants) prevented growth on a nonfermentable lactate medium and eliminated mitochondrial ATPase activity. Mutational analysis of the function of residue βR398 in *S. cerevisiae* identified the residue as non-essential (33), similar to the results obtained here.

Residue βR398 was identified as necessary to confer *E. coli* with sensitivity to the antibiotic aurovertin; mutation to His, Cys, and Trp rendered ATPase and ATP synthesis activities resistant to the antibiotic (34, 35). Furthermore, bacterial species where the equivalent residue is phenylalanine seem to be aurovertin-resistant (36). The x-ray structure of bovine mitochondrial F_1 complexed with aurovertin (37) showed that two molecules of the antibiotic were bound per F_1, one to β_{TP}, the other to β_E. In both β subunits residue βR398 contributed to aurovertin binding via hydrogen bond(s). The β_{DP}/α_{DP} hydrogen-bonding network was unperturbed.

After having established the importance of the β_{DP}/α_{DP} hydrogen-bonding network, the question about its role in the mechanism of ATP synthase remains. In the description of the original x-ray structure of F_1-ATPase, the fact that the β_{DP}/α_{DP} interface is more closed than the ones at β_{TP}/α_{TP} or β_E/α_E had led to the proposal that the catalytic site on β_{DP} might be the high affinity site (7). However, using fluorescence resonance energy transfer we could recently demonstrate that the catalytic site on β_{TP} is the high affinity site, whereas the β_{DP} site is the medium affinity site (22). Furthermore, in the present study it is shown that a nearly complete removal of the β_{DP}/α_{DP} hydrogen-bonding network has no influence on nucleotide-binding affinities at any of the three catalytic sites. It is interesting to note in this context that the molecular modeling data suggested that elimination of the hydrogen-bonding network in the βR394A/βR398A/βQ441A mutant does not significantly affect the conformation of the protein backbone of the C-terminal domains of β_{DP} and α_{DP}. Specifically, the β_{DP}/α_{DP} interface in the βR394A/βR398A/βQ441A mutant does not seem to be more "open" than in the wild-type enzyme.

Based on the localization of *mgi* mutations in *K. lactis* and their functional consequences, Wang *et al.* (32) concluded that the respective wild-type residues, including the two contributing to the hydrogen-bonding network, αF406 and βR394, might be "necessary for efficient coupling of ATP synthase, possibly by acting as support to fix the axis of rotation of the central stalk." Based on the data obtained here, we would like to propose a specific role for the β_{DP}/α_{DP} hydrogen-bonding network in coupling ATP synthesis/hydrolysis and rotation. It is important to note that in the $\alpha_3\beta_3$ ring α_{DP} is opposite of β_E. β_E carries the low affinity catalytic site, which binds the incoming MgATP during multisite ATP hydrolysis and releases the newly formed MgATP during ATP synthesis (3, 22, 23, 38, 39). It is generally assumed that MgATP binding and release are energy-linked, *i.e.* the large conformational changes in β accompanying these processes are coupled to rotation of γ (22, 39–42). In ATP hydrolysis direction, MgATP binding and the associated closing of the β_E subunit appear to drive the 80° rotation substep; a recent molecular dynamics study supports this notion (43). When β_E closes it exerts a force on γ, which has to be converted into a rotary motion of γ, instead of a lateral motion, away from the axis of rotation, which would not allow the catalytic cycle to continue (Fig. 3). As the C terminus of α_{DP} is in the direction of such a lateral motion, hydrogen-bonding it to the C terminus of β_{DP} should make it more rigid, offering greater resistance to a lateral motion of γ (for a more detailed discussion, see the legend to Fig. 3). In ATP synthesis, the situation is similar. The rotating γ subunit, powered by the flow of protons through the F_0 subcomplex, has to be kept in a position where its rotation can be translated into opening of the low affinity catalytic site and release of the newly formed MgATP.

With the exception of the αQ399A mutant, which did not assemble, none of the mutants with a reduced set of hydrogen bonds was completely inactive. In the context of the model presented here this means that even the most impaired mutants had occasionally a rotation step, probably interspersed with non-productive events where γ moved laterally away from the rotation axis.

The model proposed here is supported by the finding that the bonds at either end of the network are more important than the

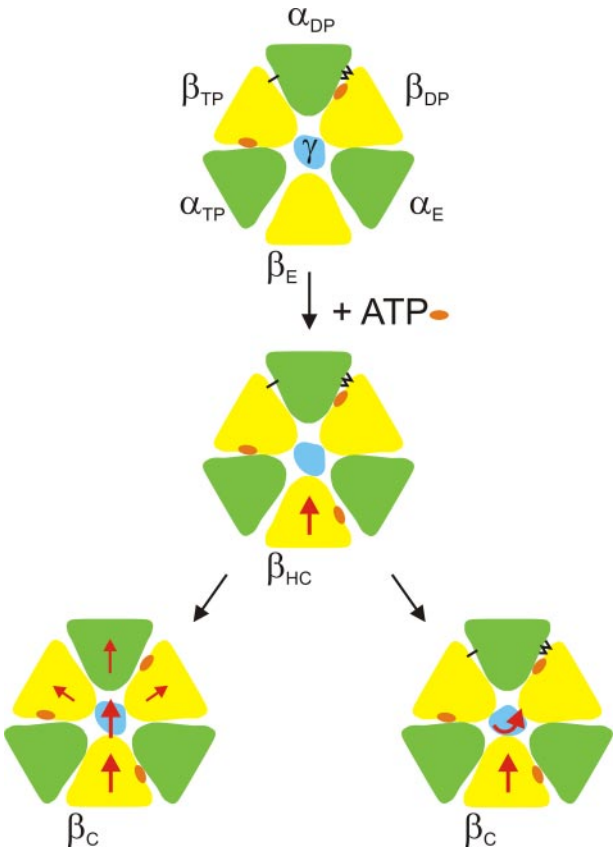

FIGURE 3. **Model of the possible role of the β_{DP}/α_{DP} hydrogen-bonding network in ATP hydrolysis.** A transection of F_1 at the level of the C-terminal domains of α and β is shown, as seen from the direction of the membrane; *green*, α subunits; *yellow*, β subunits; *blue*, γ subunit. A nucleotide bound to the catalytic site in the central domain of the respective β subunit is indicated by an *orange oval*. The *black lines* between β_{DP} and α_{DP} indicate the hydrogen-bonding network. The *single black line* between α_{DP} and β_{TP} indicates the possible hydrogen-bond(s) between the C-terminal domains of these subunits (see "Discussion"); the functional importance of the latter interaction has not yet been proven. As some of the subunit movements postulated here might be rather subtle, compared with the overall size of the F_1 subcomplex, the direction of movement of a specific subunit is indicated by a *red arrow*. The starting position (*top panel*) corresponds to the two-nucleotide x-ray structure (7) where the catalytic sites on β_{TP} and β_{DP} are filled with nucleotide, whereas the low affinity nucleotide binding site on β_E is empty and the β_E subunit is in an open conformation. MgATP binds to the open β_E site, and the site starts to close by moving the C-terminal domain toward the pseudosymmetry axis. The β subunit transiently assumes a "half-closed" conformation, "β_{HC}" (*middle panel*), similar to the conformation observed for the low affinity site in the three-nucleotide structure (20), until it finally reaches the fully closed "β_C" conformation (This β_C conformation could be very similar to the β_{TP} conformation that the subunit will assume after completion of the 120° rotation step.). Because of steric clashes, γ has to be pushed "out of the way" to allow the β subunit to close completely. In the model, this can occur either by a lateral motion in the same general direction as the "pushing" C-terminal domain of β_{HC} (*bottom left-hand panel*), or it can be translated into a rotary motion (*bottom right-hand panel*). The latter movement is the desired one, as only it will allow the overall reaction to proceed. The lateral motion will exert some pressure on the C-terminal domains of α_{DP}, β_{DP}, and/or β_{TP}. Only if these domains can move away from the pseudosymmetry axis (*bottom left*), the lateral motion can occur (it does not necessarily mean that the enzyme would disintegrate under these circumstances, because it is still held together by α/β interactions in the N-terminal domain and in the nucleotide-binding domain.). According to the model, the β_{DP}/α_{DP} hydrogen-bonding network and, possibly, the hydrogen bonds between α_{DP} and β_{TP} prevent the movement of the C-terminal domains away from the axis, thus forcing γ into a rotary instead of a lateral motion (*bottom right*).

central ones. The bonds at the end are sufficient to define the geometry of the interactions between α_{DP} and β_{DP}. The central bonds confer additional binding energy, which is, at least under the conditions applied her, not absolutely required; this appears to be another example of "overengineered" subunit-subunit interactions in ATP synthase (44).

The one or two hydrogen bonds that can be formed between the C-terminal domains of α_{DP} and β_{TP} (see Fig. 3) might play a role similar to that of the β_{DP}/α_{DP} hydrogen-bonding network. In the bovine mitochondrial enzyme, the involved residues are αE355 and βS383 (bovine numbers). In *E. coli* these residues are not conserved but have been replaced by αN358 and βE369, respectively, which could also form a hydrogen bond. Alternatively, a hydrogen bond seems possible between αN358 and βQ365. The function of these residues will be tested in an approach similar to the one described here.

Finally, it should be noted that the functional importance of the β_{DP}/α_{DP} hydrogen-bonding network gives an explanation as to why the medium affinity catalytic site has to be occupied during multisite catalysis (45). So far, only the roles of the other two sites were clearly defined. The high affinity site on β_{TP} performs catalysis, and nucleotide binding and release occur at the low affinity site on β_E. Without nucleotide bound to the medium affinity site, the β_{DP} subunit will assume an open conformation, which will prevent formation of the hydrogen-bonding network, therefore impairing catalysis.

REFERENCES

1. Leslie, A. G. W., and Walker, J. E. (2000) *Philos. Trans. R. Soc. Lond. B Biol. Sci.* **355,** 465–471
2. Noji, H., and Yoshida, M. (2001) *J. Biol. Chem.* **276,** 1665–1668
3. Weber, J., and Senior, A. E. (2003) *FEBS Lett.* **545,** 61–70
4. Wilkens, S. (2005) *Adv. Protein Chem.* **71,** 345–382
5. Dimroth, P., von Ballmoos, C., and Meier, T. (2006) *EMBO Rep.* **7,** 276–282
6. Weber, J. (2006) *Biochim. Biophys. Acta* **1757,** 1162–1170
7. Abrahams, J. P., Leslie, A. G. W., Lutter, R., and Walker, J. E. (1994) *Nature* **370,** 621–628
8. Bowler, M. W., Montgomery, M. G., Leslie, A. G. W., and Walker, J. E. (2006) *Proc. Natl. Acad. Sci. U. S. A.* **103,** 8646–8649
9. Rao, R., Al-Shawi, M. K., and Senior, A. E. (1988) *J. Biol. Chem.* **263,** 5569–5573
10. Weber, J., Wilke-Mounts, S., Lee, R. S. F., Grell, E., and Senior, A. E. (1993) *J. Biol. Chem.* **268,** 20126–20133
11. Ahmad, Z., and Senior, A. E. (2004) *J. Biol. Chem.* **279,** 31505–31513
12. Klionsky, D. J., Brusilow, W. S. A., and Simoni, R. D. (1984) *J. Bacteriol.* **160,** 1055–1060
13. Senior, A. E., Langman, L., Cox, G. B., and Gibson, F. (1983) *Biochem. J.* **210,** 395–403
14. Senior, A. E., Latchney, L. R., Ferguson, A. M., and Wise, J. G. (1984) *Arch. Biochem. Biophys.* **228,** 49–53
15. Weber, J., and Senior, A. E. (2004) *Methods Enzymol.* **380,** 132–152
16. Perlin, D. S., Cox, D. N., and Senior, A. E. (1983) *J. Biol. Chem.* **258,** 9793–9800
17. Taussky, H. H., and Shorr, E. (1953) *J. Biol. Chem.* **202,** 675–685
18. Van Veldhoven, P. P., and Mannaerts, G. P. (1987) *Anal. Biochem.* **161,** 45–48
19. Nadanaciva, S., Weber, J., and Senior, A. E. (2000) *Biochemistry* **39,** 9583–9590
20. Menz, R. I., Walker, J. E., and Leslie, A. G. W. (2001) *Cell* **106,** 331–341
21. Weber, J., Dunn, S. D., and Senior, A. E (1999) *J. Biol. Chem.* **274,** 19124–19128
22. Mao, H. Z., and Weber, J. (2007) *Proc. Natl. Acad. Sci. U. S. A.* **104,** 18478–18483
23. Scanlon, J. A. B., Al-Shawi, M. K., Le, N. P., and Nakamoto, R. K. (2007) *Biochemistry* **46,** 8785–8797
24. Nadanaciva, S., Weber, J., and Senior, A. E. (1999) *J. Biol. Chem.*, **274,** 7052–7058

25. Altschul, S. F., Madden, T. L., Schäffer, A. A., Zhang, J., Zhang, Z., Miller, W., and Lipman, D. J. (1997) *Nucleic Acids Res.* **25,** 3389–3402
26. Bowler, M. W., Montgomery, M. G., Leslie, A. G. W., and Walker, J. E. (2007) *J. Biol. Chem.* **282,** 14238–14242
27. Cabezon, E., Montgomery, M. G., Leslie, A. G. W., and Walker, J. E. (2003) *Nat. Struct. Biol.* **10,** 744–750
28. Gledhill, J. R., Montgomery, M. G., Leslie, A. G. W., and Walker, J. E. (2007) *Proc. Natl. Acad. Sci. U. S. A.* **104,** 15671–15676
29. Kabaleeswaran, V., Puri, N., Walker, J. E., Leslie, A. G. W., and Mueller, D. M. (2007) *EMBO J.* **25,** 5433–5442
30. Stocker, A., Keis, S., Vonck, J., Cook, G. M., and Dimroth, P. (2007) *Structure* **15,** 904–914
31. Clark-Walker, G. D., Hansbro, P. M., Gibson, F., and Chen, X. J. (2000) *Biochim. Biophys. Acta* **1478,** 125–137
32. Wang, Y., Singh, U., and Mueller, D. M. (2007) *J. Biol. Chem.* **282,** 8228–8236
33. Ichikawa, N., Chisuwa, N., Tanase, M., and Nakamura, M. (2005) *J. Biochem.* (*Tokyo*) **138,** 201–207
34. Lee, R. S. F., Pagan, J., Satre, M., Vignais, P. V., and Senior, A. E. (1989) *FEBS Lett.* **253,** 269–272
35. Lee, R. S. F., Pagan, J., Wilke-Mounts, S., and Senior, A. E. (1991) *Biochemistry* **30,** 6842–6847
36. Hicks, D. B., and Krulwich, T. A. (1990) *J. Biol. Chem.* **265,** 20547–20554
37. van Raaij, M. J., Abrahams, J. P., Leslie, A. G. W., and Walker, J. E. (1996) *Proc. Natl. Acad. Sci. U. S. A.* **93,** 6913–6917
38. Weber, J., Bowman, C., and Senior, A. E. (1996) *J. Biol. Chem.* **271,** 18711–18718
39. Gao, Y. Q., Yang, W., and Karplus, M. (2005) *Cell* **123,** 195–205
40. Gao, Y. Q., Yang, W., Marcus, R. A., and Karplus, M. (2003) *Proc. Natl. Acad. Sci. U. S. A.* **100,** 11339–11344
41. Yasuda, R., Noji, H., Yoshida, M., Kinosita, K., Jr., and Itoh, H. (2001) *Nature* **410,** 898–904
42. Nishizaka, T., Oiwa, K., Noji, H., Kimura, S., Muneyuki, E., Yoshida, M., and Kinosita, K., Jr. (2004) *Nat. Struct. Mol. Biol.* **11,** 142–148
43. Pu, J., and Karplus, M. (2008) *Proc. Natl. Acad. Sci. U. S. A.* **105,** 1192–1197
44. Weber, J., Wilke-Mounts, S., and Senior, A. E. (2003) *J. Biol. Chem.* **278,** 13409–13416
45. Weber, J., and Senior, A. E. (2001) *J. Biol. Chem.* **276,** 35422–35428
46. Löbau, S., Weber, J., and Senior, A. E. (1998) *Biochemistry* **37,** 10846–10853
47. Weber, J., Wilke-Mounts, S., and Senior, A. E. (2002) *J. Biol. Chem.* **277,** 18390–18396
48. Ketchum, C. J., Al-Shawi, M. K., and Nakamoto, R. K. (1998) *Biochem. J.* **330,** 707–712
49. Weber, J., Lee, R. S. F., Grell, E., and Senior, A. E. (1992) *Biochemistry* **31,** 5112–5116